



Case report

Uterine corpus tumor with neuroectodermal differentiation and frequent ganglion-like cells in a postmenopausal woman

Taku Homma^{a,*}, Takehiro Nakao^b, Toshiya Maebayashi^c, Toshiyuki Ishige^a, Hiroyuki Hao^a^a Division of Human Pathology, Department of Pathology and Microbiology, Nihon University School of Medicine, 1-30 Ohyaguchikamimachi, Itabashi, Tokyo 173-0032, Japan^b Department of Gynecology, Nihon University School of Medicine, 1-30 Ohyaguchikamimachi, Itabashi, Tokyo 173-0032, Japan^c Department of Radiology, Nihon University School of Medicine, 1-30 Ohyaguchikamimachi, Itabashi, Tokyo 173-0032, Japan

ARTICLE INFO

Keywords:

Postmenopausal woman
 Uterus
 Malignant neoplasm
 Neuroectodermal tumor
 Ganglion-like cell

1. Introduction

Uterine neuroectodermal tumors (NETs) are uterine neoplasms with a poor prognosis (Elizalde et al., 2016; Euscher et al., 2008; Novo et al., 2015; Prat et al., 2014). They are pathologically classified into 2 groups: 1) those resembling central nervous system (CNS) embryonal tumors (central-type NETs) (Euscher et al., 2008; McLendon et al., 2016; Prat et al., 2014), and 2) those resembling peripheral primitive neuroectodermal tumors/Ewing sarcomas (peripheral-type NETs) (Elizalde et al., 2016; Novo et al., 2015; Prat et al., 2014). Uterine NETs are also associated with endometrial adenocarcinomas, carcinosarcomas, and high-grade sarcomas (Prat et al., 2014). However, the pathogenesis of NETs remains unknown because of the rarity of this type of malignancy (Elizalde et al., 2016; Euscher et al., 2008; Novo et al., 2015; Prat et al., 2014). Here, we present a patient with a rare uterine NET comprising frequent ganglion-like cells.

2. Case report

A 62-year-old Japanese woman was receiving medications for cellulitis and deep vein thrombosis of her right and left lower extremities. During follow-up visits for these ailments, contrast-enhanced computed tomography (CT) revealed a solid uterine tumor exhibiting heterogeneous enhancement (Fig. 1A) with multiple swollen intra-pelvic and para-abdominal aortic lymph nodes. The uterine mass exhibited hypointensity and high intensity on T1-weighted (Fig. 1B) and T2-weighted (Fig. 1C) pelvic magnetic resonance imaging, respectively. As

the patient also complained of vaginal bleeding, she was admitted to our hospital for further examinations. Blood tests revealed elevated levels of the following tumor markers: carcinoembryonic antigen, 14.8 ng/mL (normal, < 5 ng/mL); carbohydrate antigen (CA) 19-9, 1300 U/mL (normal, < 40 U/mL); CA125, 68 U/mL (normal, < 35 U/mL); and neuron-specific enolase (NSE), 77.4 ng/mL (normal, < 16.3 ng/mL). Endometrial biopsy was performed, and the specimen was diagnosed as a leiomyosarcoma. There were para-abdominal aortic lymph node metastases (Fig. 1D), resulting hydronephrosis of both kidneys (Fig. 1E). One month later, the patient underwent total abdominal hysterectomy (TAH), bilateral salpingo-oophorectomy (BSO), and partial omentectomy. However, her renal dysfunction did not improve and her general condition gradually worsened to a level that precluded postoperative chemotherapy or radiation therapy. She died of multiple organ failure 2 months after the discovery of the tumor.

3. Pathologic findings

The resected uterus comprised almost entirely of a milky-whitish tumor with necrosis, measuring 15 × 9 cm in size (Fig. 2A). The tumor was histopathologically classified as a highly malignant cellular neoplasm (Fig. 2B) and was mainly composed of small naked neoplastic cells (Fig. 2C). The following additional histological components were noted: atypical ganglion-like cells with a fibrillary background (Fig. 2D), endometrial adenocarcinoma with squamous differentiation (Fig. 2E), rhabdoid-like cells (Fig. 2F), atypical spindle cells resembling skeletal muscular cells, and an atypical cartilaginous component. The

* Corresponding author.

E-mail address: homma.taku@gmail.com (T. Homma).

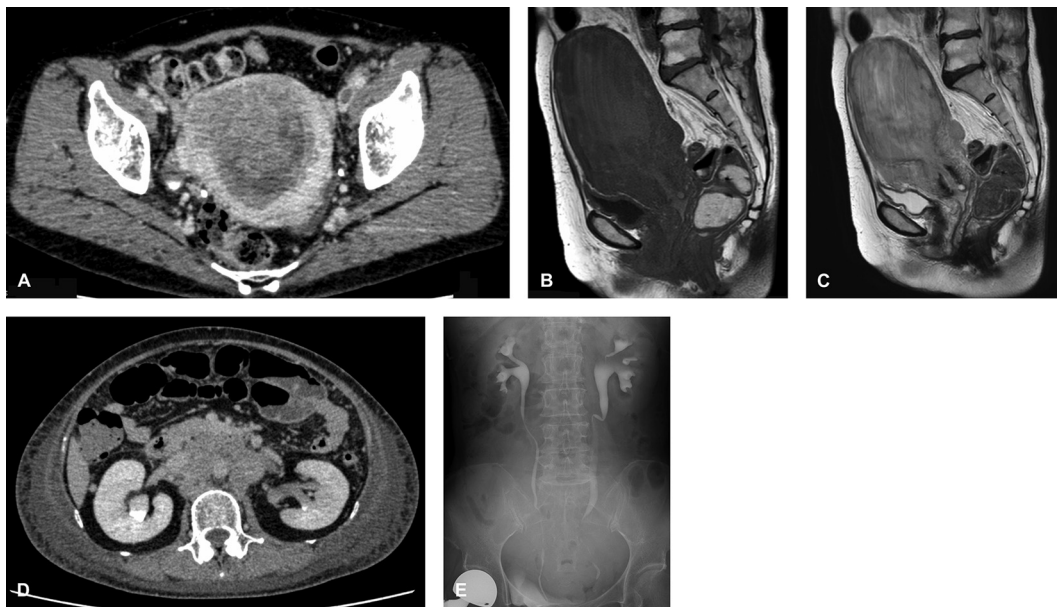


Fig. 1. Radiological features of the uterine tumor and hydronephrosis. Contrast-enhanced computed tomography (CT) showed the large solid uterine tumor with heterogeneous enhancement (A). Magnetic resonance imaging showed the uterine tumor with slightly heterogeneous hypointensity on T1-weighted imaging (B) and hyperintensity on T2-weighted imaging (C). CT showed prominent para-aortic lymph node metastases (D), resulting bilateral hydronephrosis (drip infusion pyelography; E).

component comprising atypical ganglion-like cells with a fibrillary background occupied approximately 92% of the uterine tumor. The neoplasm directly infiltrated the parametrium and had metastasized to both ovaries as well as the major omentum.

Immunohistochemically, the small naked neoplastic cells showed varying degrees of immunoreactivity for vimentin, CD99, CD56, S100, synaptophysin (Fig. 3A), alpha-smooth muscle actin (α -SMA), neurofilament (NF), and chromogranin A (CGA). Both the atypical ganglion-like cells and fine fibrillary background were positive for synaptophysin (Fig. 3B), S100, CD56, CD99, and NF. The atypical ganglion-like cells were also positive for CGA. A few neuronal nuclei (NeuN)-positive atypical ganglion-like cells and glial acidic protein (GFAP)/oligodendrocyte lineage transcription factor 2 (Olig2)-positive fibrillary astrocytes were also detected (Fig. 3C). The endometrial adenocarcinoma with a squamous differentiation component was diffusely positive for cytokeratin (CK) AE1/AE3 (Fig. 3D) and epithelial membrane antigen (EMA), and was focally positive for vimentin. The squamous differentiation component showed p40 immunoreactivity. The rhabdoid-like cells revealed immunoreactivity for vimentin, synaptophysin, CGA, and NF, suggesting small ganglion cells, whereas it was negative for S-100, human melan black-45 (HMB-45), GFAP, Olig2, NeuN, epithelial markers (cytokeratin [CAM5.2], EMA, and pan-CK [AE1/AE3]), and muscular markers (desmin, myogenin, and α -SMA). Nuclear INI1 protein immunoreactivity was preserved in the tumor, including in the rhabdoid-like cells (Fig. 3E). α -SMA-positive atypical spindle cells were intermingled with the epithelial and neuronal components. The MIB-1 labeling index was $> 50\%$ in the small round neoplastic cells (Fig. 3F) and approximately 20% in the ganglion-like cells with fibrillary background. No neoplastic cells were positive for melanoma (HMB-45 and melan-A) or skeletal muscle (desmin and myogenin) markers. Based on these features, the pathological diagnosis was uterine NET with frequent ganglion-like cells.

Widespread dissemination of the uterine NET was found on autopsy. The uterine neoplastic cells had metastasized or disseminated to the lungs, liver, appendix vermiformis, urinary bladder, ureters, Douglas' pouch, peritoneum, mesentery, and lymph nodes (para-aortic, peritracheal, and peri-pancreatic). The metastatic cells were mainly comprised of NET with ganglion-like cells and a fibrillary background;

however, no metastases of the carcinomatous or sarcomatous components were noted. Both kidneys showed mild hydronephrosis that was secondary to tumor spreading. No remarkable changes were noted in the heart, alimentary tract, pancreas, gallbladder, thyroid gland, or adrenal glands.

4. Discussion

Uterine NET is rare; only 69 patients with this tumor type have been reported in the English-language literature to date (Table 1). Clinically, uterine NET usually occurs in postmenopausal women and presents with vaginal bleeding (Euscher et al., 2008; Prat et al., 2014). Indeed, 78.7% of the patients with uterine NETs listed in Table 1 experienced vaginal bleeding, and 72.9% of them were over 40 years old. Approximately 50% of these uterine neoplasms are found to have metastasized to the extra-uterine tissues/organs at diagnosis (Prat et al., 2014). The major metastatic sites of uterine NETs are the lymph nodes via the lymphatic system (Daya et al., 1992; Odunsi et al., 2004; Shah et al., 2009; Park et al., 2007; Elizalde et al., 2016) and lungs/liver via the vasculature (Bartosch et al., 2011; Gersell et al., 1989; Hendrickson and Scheithauer, 1986; Shah et al., 2009; Sinkre et al., 2000; Yi et al., 2015), as was also observed in our patient. Although the standard treatment for uterine NETs normally involves surgery (TAH + BSO) with or without chemotherapy and/or radiotherapy (Elizalde et al., 2016), we recommend that lymph node dissection also be performed when possible. However, the necessity of omentectomy in patients with uterine NETs remains unconfirmed because it has been performed in too few patients who underwent TAH + BSO (Table 1).

As for the prognosis of patients with uterine NETs, Euscher et al. (2008) reported a mortality rate of 47% in their largest uterine NET series; furthermore, the 2-year survival rate of postmenopausal patients with uterine NET was reported to be approximately 30% (Elizalde et al., 2016; Prat et al., 2014). Consistent with previous reports, our patient was also a postmenopausal woman with minimal vaginal bleeding, and had a uterine tumor with lymphadenopathy at the time of diagnosis. She died 2 months after the uterine mass was diagnosed despite undergoing TAH, BSO, and omentectomy; however, lymph node dissection was not possible. As such, our patients' uterine NET was consistent

Download English Version:

<https://daneshyari.com/en/article/8781014>

Download Persian Version:

<https://daneshyari.com/article/8781014>

[Daneshyari.com](https://daneshyari.com)